Atmos. Meas. Tech. Discuss., doi:10.5194/amt-2016-5, 2016
Manuscript under review for journal Atmos. Meas. Tech.
Published: 1 February 2016

Atmospheric Measurement Techniques Discussions

Comparison of GPS tropospheric delays derived from two consecutive EPN reprocessing campaigns from the point of view of climate monitoring

Zofia Baldysz[1], Grzegorz Nykiel[1], Andrzej Araszkiewicz[1], Mariusz Figurski[1], and Karolina Szafranek[1]
[1]Military University of Technology, Faculty of Civil Engineering and Geodesy, Warsaw, Poland
Correspondence to: Zofia Baldysz (zofia.baldysz@wat.edu.pl)

Abstract. The main purpose of this research was to acquire information about consistency of the ZTD (Zenith Tropospheric Delay) linear trends and seasonal components between two consecutive GPS reprocessing campaigns. The analysis concerned two sets of the ZTD time series which were estimated during EPN (EUREF Permanent Network) reprocessing campaigns according to 2008 and 2015 MUT LAC (Military University of Technology Local Analysis Centre) scenarios. Firstly, Lomb-Scargle periodograms were generated for 57 EPN stations to obtain characters of oscillations occurring in the ZTD time series. Then, the values of seasonal components and linear trends were estimated using the LSE (Least Square Estimation) approach. The Mann-Kendall Trend Test was also carried out to verify the presence of linear long term ZTD changes. Finally, differences in seasonal signals and linear trends between these two data sets were investigated. In case of spectral analysis, amplitudes of the annual and semiannual periods were almost exactly the same for both reprocessing campaigns. Exceptions were found for only a few stations and they did not exceed 1 mm. The estimated trends were also similar. However, in case of reprocessing performed in 2008, the trends values were generally higher than the values from the other one. All these analyses were conducted for two lengths of the ZTD time series: a shortened 16-year series, and a full 18-year one. In general, shortening of the analysed period of time resulted in decrease of the linear trends values of about 0.7 mm/decade. This was confirmed by analyses based on two data sets.

1 Introduction

Climate plays a key role in shaping the environment in which man lives. It is a changing set of interconnected phenomena, and therefore requires continuous research aimed to evaluate the current state of the atmosphere and predict its future changes. Water vapour is one of the most important natural greenhouse gases. It is responsible for the Earth energy balance (Soden and Held, 2006) and it is one of the major factors that affect the climate changes. The exact extent of its impact on the heat-trapping quantity is still under discussion, however, it was already demonstrated that it is responsible for about 60-70% of the Earth's surface temperature increase (COST, 2012). Water vapour also plays a major role in shaping the dynamic processes in the atmosphere and the hydrological cycle. All these factors motivate scientists to monitor the variability of its content in the atmosphere. There are several methods based on the results of measurements made by means of radiosondes, sun photometers or satellite devices (e.g. GOME, GOME-2) which enable to determine the amount of water vapour in the

Atmos. Meas. Tech. Discuss., doi:10.5194/amt-2016-5, 2016
Manuscript under review for journal Atmos. Meas. Tech.
Published: 1 February 2016

Atmospheric Measurement Techniques Discussions

troposphere (IWV, Integrated Water Vapour). However, due to increased need for more climatological data geodetic techniques (like Global Navigation Satellite Systems, Doppler Orbitography and Radiopositioning Integrated by Satellite, Very Long Baseline Interferometry) are used for this purpose as well. Among them, GPS observations have started to play a significant role in this task. This is mainly caused by the fact that GPS stations, regardless of weather conditions, provide continuous data of high temporal and spatial resolution. In practice, scientists use the GPS signal propagation delay which is caused by the physical properties of the neutral part of the atmosphere. Advanced processing of the GPS observations enables to determine its value with very high accuracy. It was agreed to express this phenomenon in the zenith direction and call it the Zenith Total Delay (ZTD). It includes delays caused by the hydrostatic (ZHD, Zenith Hydrostatic Delay) and the wet (ZWD, Zenith Wet Delay) parts of the atmosphere. In principle, ZTD reflects the state of the troposphere, so it is possible to use its value, together with selected meteorological parameters, to estimate IWV (Bevis et al., 1992). Then, using long term observations, it is also possible to study its changes in time (e.g., Emardson et al., 1998; Nilsson and Elgered, 2008; Wang and Zhang, 2009), which constitutes the beginning of its use in climate research. However, it is worth to notice here that IWV obtained from ZTD and meteorological parameters contains errors. They are a result of the uncertainty of: ZTD estimation, ZHD modelling, the method of interpolation (in all those cases when meteorological parameters have to be interpolated from e.g. weather models) and from the ZWD to IWV conversion formula (e.g., Hagemann et al., 1992; Bock et al., 2007; Van Malderen et al., 2014). Therefore, several studies have been conducted to find the best methods of reducing these errors and uncertainties. They focused mainly on the homogenization of ZTD time series (e.g., Hagemann et al., 1992; Bock et al., 2014) or using different methods of interpolation (Wilgan et al., 2014). One has to keep in mind, that GPS achieved full operational capability in 1995. Since that time processing strategy has been changed several times. As in other researches, also in climate studies the analyzed data should be as homogeneous as possible (Bengtsson et al., 2004). Such requirement can be met by using reprocessed data because they minimize errors which result from the switching calculation strategy. Nowadays, their potential as a source of information for climate research is constantly growing (e.g., Pacione et al., 2014). Moreover, adopted processing strategy could also affect the estimated ZTD values. This is particularly important, when changes in the water vapour content are very small and any mismodelling of the tropospheric parameters could also distort the estimated trend. As it was already presented by Nilsson and Elgered (Nilsson and Elgered, 2008) or Baldysz (Baldysz et al., 2015), extending the analyzed period even for two additional years could change the nature of the trend. This complies with the need of climate research which requires long time series. ZTD shows correlation with time-dependent temperature (Guerova, 2013) or water vapour content (Yong et al., 2008). Its size and seasonal variability are related to such factors as latitude, altitude above sea level or distance from big masses of water. Therefore, it could also provide information about the prevailing local weather conditions (Jin et al., 2007). Based on these facts and taking into account that ZTD is a direct GPS product, the authors decided to focus on this parameter. To investigate the impact of adopting the GPS processing strategy on the ZTD parameter, and therefore on climate applications of ZTD, the authors compared two different data sets. The first of them came from the first EPN (EUREF Permanent Network) (Bruyninx, 2004) reprocessing campaign (called here Repro1), extended according to the same strategy to 2013. These data were already analyzed by Baldysz (Baldysz et al., 2015). The second one was obtained from the latest EPN reprocessing campaign (called here Repro2). Due to the fact, that the ZTD parameter should reflect the real amount of delay caused by the

Atmos. Meas. Tech. Discuss., doi:10.5194/amt-2016-5, 2016
Manuscript under review for journal Atmos. Meas. Tech.
Published: 1 February 2016

Atmospheric Measurement Techniques Discussions

troposphere, theoretically ZTD estimated during both reprocessing campaigns should be the same. Consequently, the designed oscillations and linear trends should also be identical for time series from exactly the same period of time (from the Repro1 and Repro2 campaigns). However, the use of various software and computing strategy, including models and parameters, may have influence on its value. In this connection, the authors decided to analyze the differences between these two solutions. Analyses were conducted for two lengths of ZTD time series: a shortened 16-year one to maximize spatial distribution of stations (57 stations), and a full 18-year one to ensure the maximum length of the analyzed period of time (28 stations).

2 Analyzed data

The value of ZTD is a consequence of electromagnetic wave delay which is caused by refraction and attenuation in the troposphere. The value of this delay is given in the zenith direction and is defined in the following formula (Bevis et al., 1992):

$$ZTD = c\tau = 10^{-6}\int_0^{\infty} N(s)ds \tag{1}$$

where c is the speed of light in vacuum, τ is the delay measured in the unit of time and N is the neutral atmospheric refractivity (Davis et al., 1985):

$$N = k_1\rho + k_2\frac{P_w}{Z_w T} + k_3\frac{P_w}{Z_w T^2} \tag{2}$$

where ki (i=1, 2, 3) is a constant, ρ is the total mass density of the atmosphere, P_w is the partial pressure of water vapour, Z_w is the compressibility factor and T is the temperature in Kelvin.

Delay caused by hydrostatic part of the atmosphere is given by the integral of the first term of Eq. 2 while the influence of the wet part of atmosphere is given by the integral of the remaining two terms of Eq. 2. During GPS observation, most of the satellites which are tracked by receivers, are not in the zenith direction. Therefore, the value of delay between each pair of a satellite and an antenna is calculated not in the zenith but in a slant direction (STD, Slant Tropospheric Delay). Hence, it depends on the satellite's zenith distance. For relating STD to ZTD, it is necessary to use mapping functions which are approximately equal to 1/sine, where e is elevation angle. However, for precise position determination, this approximation is not sufficient and the following function given by Marini (Marini, 1972), and normalized by Herring (Herring, 1992) has to be used:

$$mf(e) = \frac{1+\frac{a}{1+\frac{b}{1+c}}}{\sin e + \frac{a}{\sin e+\frac{b}{\sin e+c}}} \tag{3}$$

where e is the elevation angle and a, b, and c are coefficients which relate to the state of the atmosphere (determined differently for different mapping functions). Mapping functions are used separately for hydrostatic and wet parts of delay. The total value of delay in the zenith direction can thus be expressed as:

$$ZTD = ZHD \times mf(e)_{hyd} + ZWD \times mf(e)_{wet} \tag{4}$$

Atmos. Meas. Tech. Discuss., doi:10.5194/amt-2016-5, 2016
Manuscript under review for journal Atmos. Meas. Tech.
Published: 1 February 2016

where $mf(e)_{hyd}$ is a mapping function for hydrostatic delay and $mf(e)_{wet}$ is a mapping function for wet delay. ZTD described by the above formulas is one of many unknowns which are estimated during position determination. For this reason it may be affected by adopting various calculations strategies (e.g., Ning and Elgered, 2012). Therefore obtaining the most reliable value of ZTD during processing of GPS observations is one of the major tasks for scientists who focus on the atmospheric research. In this paper, two different reprocessing campaigns of EPN were compared. This allows to identify how updating of the GPS processing strategy affects the tropospheric parameters.

EPN is a network of permanent GNSS stations built on the basis of and as a densification of the IGS global network (International GNSS Service) in Europe. It has been operated continuously since 1996. During this time various algorithms, models, parameters and software were involved to process GPS data collected by the stations. This resulted in collecting and archiving inhomogeneous sets of data which in consequence prevented from conducting proper analyses of long time series. Such state of affairs led to decisions made in 2008 and in 2013 about recalculating all data (from the level of observation files) according to one coherent strategy. This task was done inter alia by the Military University of Technology, one of the EPN Analysis Centres (MUT AC) in the frame of a special EUREF project called "EPN reprocessing". The first campaign (2008) (Figurski et al., 2009; Sohne et al., 2010) covered all EPN stations which were operated in the EPN network from January of 1996 through December of 2007. The second campaing (2015) covered all EPN stations which were operated from January of 1996 through December of 2014. To align the analyzed periods, the authors decided to recalculate the data from January of 2008 through December of 2013 according to the Repro1 strategy. This ensured the maximum coherence during comparison of the data from these two reprocessing campaigns.

Over the years between the Repro1 and the Repro2 campaigns, the knowledge and capabilities of physical modelling changed. There was no assumption about homogeneity between both campaigns. Consequently, calculation strategies in both reprocessing campaigns were not similar and could result in differences in ZTD values. The first major difference between Repro1 and Repro2 was in software that was used. Bernese 5.0 software (Dach et al., 2014) was used in Repro1 while GAMIT 10.5 software (King et al., 2010) for the Repro2 calculations. Both solutions were based on the GPS system and the relative approach. However, reprocessed IGS orbits (IGS repro1) were used in Repro1 while reprocessed orbits provided by CODE in 2013 were used in Repro2 . This implies that the solutions were expressed in different reference frames (Repro1 in IGS05 and Repro2 in IGb08). Consequently, the used antenna models were changed. Besides the alignment to the specific reference frame, the source of PCC (Phase Centre Correction) was also different. IGS type mean and EPN individual calibrations were used in Repro1 while only the IGS type mean calibrations were used in the Repro2 campaign. In terms of geophysical phenomena modeling, only the ocean tidal loading model (based on FES2004, Finite Element Solution 2004) was applied in Repro1. In Repro2, the FES2004 as well as atmospheric tides based on the ECMWF CMT (ECMWF European Centre for Medium Range Weather Forecasts Convective Momentum Transport) and atmospheric non tidal loadings based on the NCEP (National Centre for Environmental Prediction) were taken into account. These models were applied to data processing on the observation level, as it was described by Tregoning and Watson (Tregoning and Herring, 2006). Next to geophysical phenomena, also the impact of ionosphere on phase measurements, was removed in various ways. In the first reprocessing campaign, only the first order ionospheric effects were eliminated by using a linear combination. In the latest one, all three orders of ionospheric corrections

Atmos. Meas. Tech. Discuss., doi:10.5194/amt-2016-5, 2016
Manuscript under review for journal Atmos. Meas. Tech.
Published: 1 February 2016

Atmospheric Measurement Techniques Discussions

Table 1. Comparison of the processing strategies of the Repro1 and the Repro2 campaigns

	Repro1 campaign	**Repro2 campaign**
software	Bernese 5.0	Gamit 10.50
GNSS system	GPS	Gamit GPS
observations	double differences	double differences
antenna calibration	absolute and individual	absolute
elevation mask	3°	5°
troposphere alignment	ZTD based on weekly coordinates	ZTD based on daily coordinates
mapping functions	Niell Mapping Functions	Vienna Mapping Functions 1
ionosphere modeling	iono-free	iono-free, II-order and III-order effects modeled based on ionosperic maps (CODE) and IGRF11 model
ocean loadings	FES2004	FES2004
tidal atmospheric loadings	none	sourced from ECMWF
nontidal atmospheric loadings	none	sourced from NCEP

were modeled according to Petrie (Petrie et al., 2010). Another discrepancy was in the adopted elevation mask: 3 degree in Repro1 and 5 degree in Repro2. Moreover, during the first reprocessing campaign ZTD solutions were fixed to weekly coordinates while during the second one they were fixed to daily coordinates. The differences mentioned above are not directly related to troposphere modeling. However, accuracy of GPS-derived ZTD is affected by elevation-angle-dependent errors which could be caused by atmospheric mapping functions (Stoew et al., 2007), antenna phase center variations (Schmid et al., 2007) or signal multipath (Elósegui et al., 1995). Parameters which are directly related to the state of the troposphere have more immediate impact. From this point of view, the biggest differences between Repro1 and Repro2 occurred in mapping functions. In Repro1, Niell Mapping Function (NMF) (Niell, 1996), with coefficients for hydrostatic and nonhydrostatic components obtained from radiosondes profiles, was used. Another approach was adopted in the second reprocessing campaign. Instead of NMF, Viena Mapping Function 1 (Boehm et al., 2006), with coefficients for hydrostatic and nonhydrostatic components delivered from ECMWF (European Centre for Medium Range Weather Forecasts), was used. Estimation of the influence of various mapping functions on troposphere modeling was the goal of several studies (e.g., Tesmer et al., 2007; Vey et al., 2006). However, these researches were mostly focused on coordinates or short term ZTD time series, and therefore it is difficult to conclude about their impact on climate applications. The adopted processing strategies for both reprocessing campaigns are summarized in Table 1.

The described above two sets of data were derived from 57 EPN stations which have been operated continuously since at least 1998. In case of the EPN network, the longest possible time series come from the stations which were launched simultaneously in the beginning of 1996. However, there are only 30 such stations. This number does not provide adequate spatial distribution

Atmos. Meas. Tech. Discuss., doi:10.5194/amt-2016-5, 2016
Manuscript under review for journal Atmos. Meas. Tech.
Published: 1 February 2016

Atmospheric Measurement Techniques Discussions

which is necessary for analyses of temporal and spatial changes of tropospheric parameters in such a big area. Therefore, the authors decided to analyze 16-year ZTD time series for both reprocessing campaigns (January of 1998 through December of 2013). Such assumption doubles the number of stations which could be involved and therefore compared in our analysis. Time series from stations which were also operated before 1998, were shortened to the period of time from January of 1998 through December of 2013, to ensure maximum homogeneity of data. Full 18-year ZTD time series were also studied. This approach was similar to the case of the previous study (Baldysz et al., 2015) and enabled to investigate whether the nature of changes that the additional two years introduce is the same for both campaigns.

Besides the length of the ZTD time series, their quality is particularly important for climate studies. This is mainly due to the fact, that the investigated changes can be very small. Such situation implies, that they shouldn't be disturbed by any additional pollution like gaps in time series or big number of outliners. Therefore, ZTD data screening was conducted in both data sets: all outliners that exceeded two standard deviations ($2\,\sigma$) were removed. Furthermore, data availability analysis was performed - the real numbers of data were compared to the theoretical numbers of data (theoretical maximum number of hourly solutions available from a station). Stations with less than 90 % of the theoretical number of data were removed. This requirement had to be met by each station in both sets of data (from the Repro1 and Repro2 campaigns). Only two of all the analyzed stations, ANKR (Turkey) and SVTL (Russian Federation), had to be excluded from further analysis. Distribution of stations included in the analysis is shown in Fig. 1.

3 Analysis of ZTD time series

Seasonal variations in the ZTD time series are important in climate analyses. On the one hand, they carry information about prevailing weather conditions in a given region. On the other hand, assuming their occurrence is important when the linear trend is determined using the Least Square Estimation (LSE) approach. To ensure the homogeneity of the compared results (from the Repro1 and Repro2 campaigns), the authors adopted exactly the same methodology as in case of the previous work (Baldysz et al., 2015) where data from the Repro1 campaign were analyzed. Information concerning oscillations in the ZTD time series was obtained by preparing the Lomb-Scargle periodograms for every station. According to this method, the frequency spectrum is estimated by fitting the linear squares of sine and cosine model to the observed time series (Lomb, 1976):

$$x(t_i) = a\cos(\omega t_i - \Theta) + b\sin(\omega t_i - \Theta) + n_i \tag{5}$$

where $x(t_i)$ is the observed time series at time t_i, a and b are constant amplitudes, ω is the angular frequency, Θ is the additional phase (required for the orthogonalization of the sine and cosine model functions when the data are unevenly spaced) and n_i is the noise at time t_i. Based on this method, the main frequencies in the ZTD time series were found. The periodograms were prepared for both sets of data (Repro1 and Repro2). Similarly as in the previous work, the authors removed the annual oscillation from the signal to investigate the smaller amplitude oscillations. Waveforms of periodograms obtained for the same stations match each other almost perfectly. Therefore, the authors present results for the most recent studies (Repro2). Figure 2a presents examples of periodograms for 5 stations: GRAS (France), GLSV (Russian Federation), SFER (Spain), MAS1

Atmos. Meas. Tech. Discuss., doi:10.5194/amt-2016-5, 2016
Manuscript under review for journal Atmos. Meas. Tech.
Published: 1 February 2016

Atmospheric Measurement Techniques Discussions

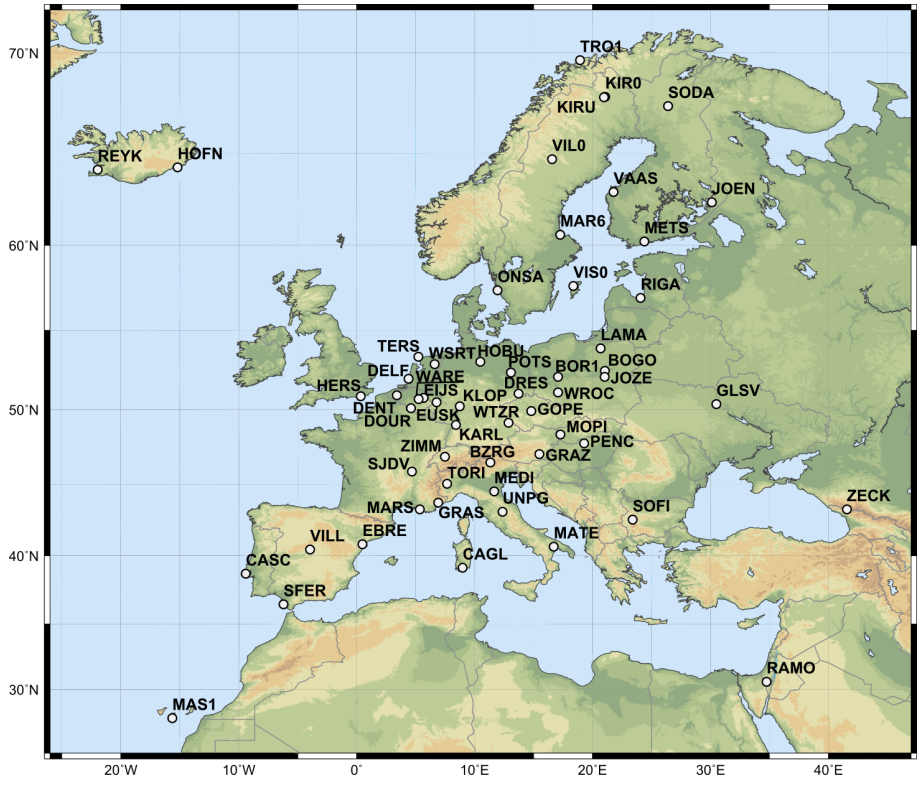

Figure 1. Distribution of stations with 16-year ZTD time series included in the analysis.

(Spain) and RAMO (Israel). The results of the seasonal components determination for the whole signal spectrum are presented in Fig. 2a (top). The periodograms for the same stations for the signal after removing the annual period are presented in Fig. 2a (bottom). Every station had a strong annual signal which is caused by the annual weather oscillation (the highest temperature in summer and the lowest temperature in winter) characteristic for mid-latitudes. For great majority of stations, a distinct semi-annual oscillation was also noticed. For some of the analyzed stations ter-annual and even quarto-annual signals were found (e.g. MAS1 station). Characteristic oscillations with about 640 days period and about 5.0 mm amplitude (Fig. 2b) were found for a group of stations located in the northern Scandinavia (TRO1, KIRU, KIR0, SODA, VIL0). Their occurrence can be caused by various phenomena. However, the authors assume that they are probably related to similar geographic location and this effect is still under investigation. Periodograms are presented for periods of not more than two years in order to improve their readability. They were originally prepared for investigating lower frequencies (even four year ones), however, such frequencies were not observed in the ZTD time series over Europe, or they were not sufficiently clear. The trend value was estimated by means of the LSE method taking into account results obtained from the Lomb-Scargle periodograms (occurance of annual, semiannual, ter-annual and quarto-annual oscillations). The values of the linear trends determined by the LSE approach were very small for some stations, therefore the authors performed the Mann-Kendall trend test (Mann, 1945; Kendall and Stuart,

Atmos. Meas. Tech. Discuss., doi:10.5194/amt-2016-5, 2016
Manuscript under review for journal Atmos. Meas. Tech.
Published: 1 February 2016

Atmospheric Measurement Techniques Discussions

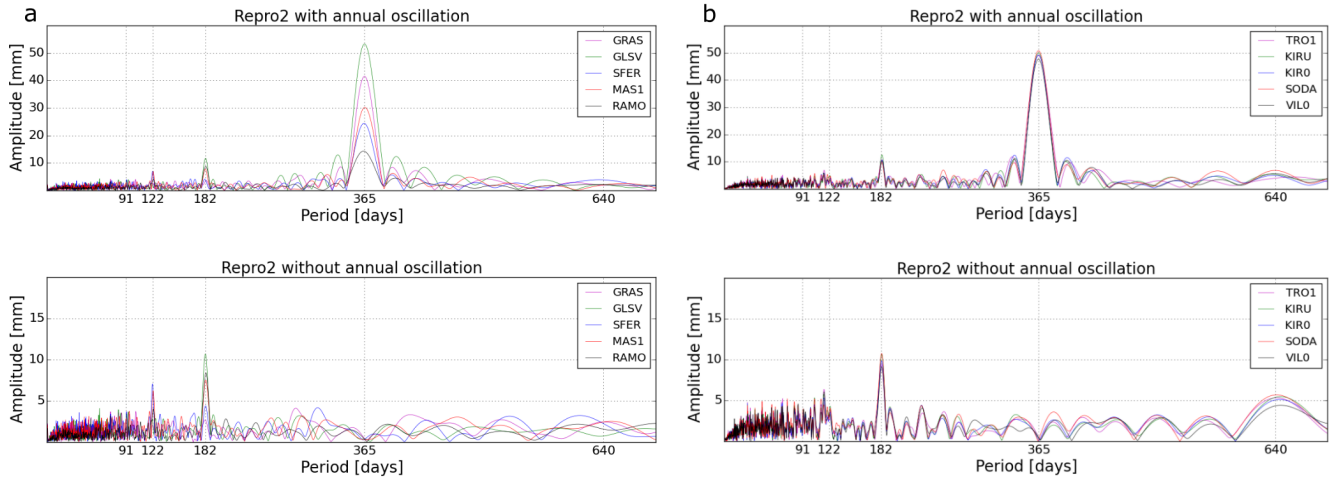

Figure 2. Lomb-Scargle periodograms for GRAS (a), GLSV (a), SFER (a), MAS1 (a) and RAMO (a) stations with the annual oscillation (top) and without it (bottom), and Lomb-Scargle periodograms for TRO1 (b), KIRU (b), KIR0 (b), SODA (b) and VIL0 (b) stations with the annual oscillation (top) and without it (bottom), based on the Repro2 campaign.

1970) to confirm their presence in the time series. All calculations were conducted according to the following formula:

$$S = \Sigma_{i=1}^{n-1}\Sigma_{j=i+1}^{n} sign(X_j - X_i) \qquad Sign(X_j - X_i) = \begin{cases} 1 & \text{if } (X_j - X_i) > 0 \\ 0 & \text{if } (X_j - X_i) = 0 \\ -1 & \text{if } (X_j - X_i) < 0 \end{cases} \tag{6}$$

where X_i andX_j are the time series while $i = 1, 2, 3 \ldots n-1$ and $j = i+1, i+2, i+3, .., n$. S, the statistical factor, returns information about the character (negative or positive) and whether the trend in the time series is strong and clear or it is rather small and not significant (the higher value of S, the higher value of the linear trend). In this paper, negative results of the Mann-Kendall trend test (trend unconfirmed) are marked as 'False', and positive results (trend confirmed) are marked as 'True'.

4 Results of seasonal analysis

Seasonal analyses were performed on the 16-year ZTD time series to ensure higher spatial distribution. As it was already mentioned in the previous section, both reprocessing campaigns gave very similar results. In more detail: the average value of the annual oscillation from Repro1 was 46.7 mm and 46.3 mm from Repro2. In both data sets, the highest amplitude of the annual period was found for the same station (TORI, Italy). Its value of 63.3 mm was exactly the same for both campaigns. The lowest value of the annual oscillation was found for the RAMO station (Israel) and it was 13.7 mm and 14.1 mm for Repro1 and Repro2, respectively. Generally, the differences between the estimated amplitudes of the annual periods were lower than

Atmos. Meas. Tech. Discuss., doi:10.5194/amt-2016-5, 2016
Manuscript under review for journal Atmos. Meas. Tech.
Published: 1 February 2016

Atmospheric Measurement Techniques Discussions

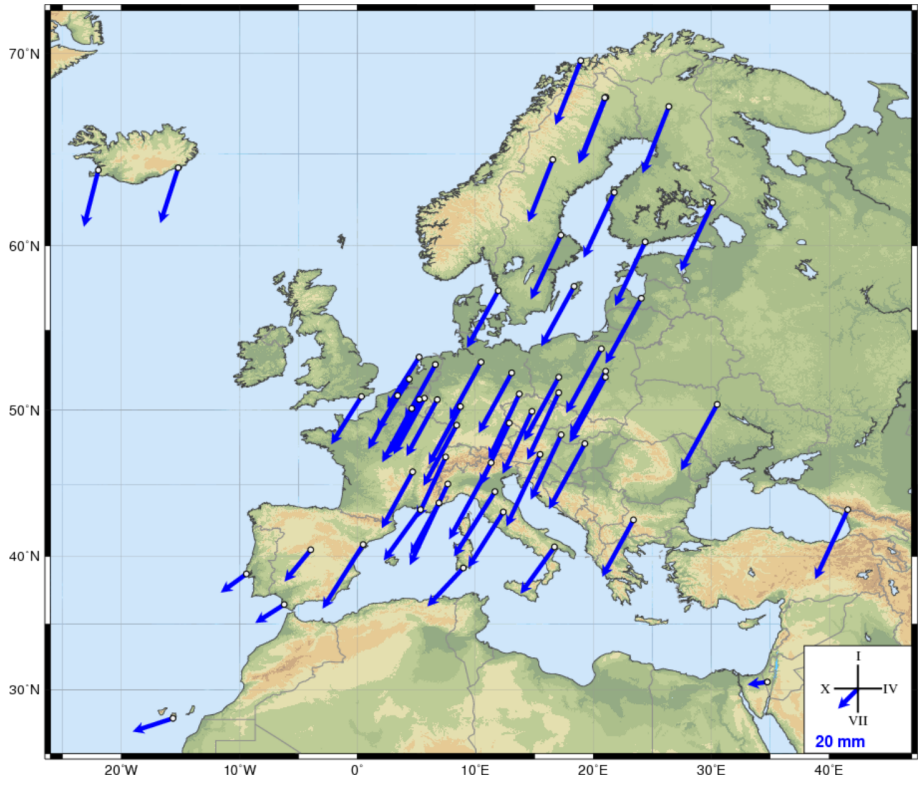

Figure 3. Amplitude and phase shift for the annual oscillation for the ZTD time series derived from the Repro2 campaign.

1 mm, except for 5 stations: DELF (the Netherlands), HOFN (Iceland), REYK (Iceland), TERS (the Netherlands) and WSRT (the Netherlands) where the differences equaled to 1.1 mm, 1.3 mm, 1.1mm, 1.3 mm and 1.2 mm, respectively. The highest amplitude of the semiannual periods was also found for the same station (JOEN, Finland) in both campaigns. Its value differed slightly and was 11.9 mm in Repro1 and 12.1 mm in Repro2. There was also no significant difference in phase for the seasonal component. In both campaigns the maximum of ZTD at 52 stations occurred on the same day of the year. A small phase shift (not more than 4 days) was found for only 5 stations: DELF (the Netherlands), MAS1 (Spain), SODA (Finland), VILL (France), and VIL0 (Iceland). Even then, the mean value of the maximum ZTD was equal in both campaigns and occured on the 214^{th} day of the year. Due to strong similarity of the results, only Repro2 was shown in Fig. 3. In Europe, the maximum temperature, which is correlated with water vapour, occurrs in late July and early August. However, it can be clearly seen that there are differences between regions. In the Mediterranean area, the maximum value of ZTD occurred on a later date than in areas in northern Europe. This is probably due to the fact that during the summer the Sun is higher above the horizon in the regions closest to the Tropic of Cancer. In these areas, the Sun supplies energy for the longest period of time (compared to the regions surrounding the Arctic Circle), intensively heating them. All results are presented in Table 2 in Appendix A. Information obtained from seasonal analyses, supplemented by the mean ZTD value, could be useful during investigation of prevailing weather conditions. It results from the correlation between the temperature and the ZTD value. Consequently, high

Atmos. Meas. Tech. Discuss., doi:10.5194/amt-2016-5, 2016
Manuscript under review for journal Atmos. Meas. Tech.
Published: 1 February 2016

values of the ZTD mean are correlated with high content of water vapor in the atmosphere. It indicates that at a given region either the high content of water vapor in the atmosphere is constant, or the humidity is very high, however, only seasonally. Complementing this information with the value and nature of the annual amplitude enables to investigate the type of climate at given station (see Table 2 in Appendix A for information about the mean value of ZTD for every station). Ranges of various climatic zones may slightly vary . Nevertheless, it is possible to indicate areas which are specific for them. The southern part of Europe, which is within the influence of the Atlantic Ocean and the Mediterranean Sea, is located in the humid subtropical climate zone. It is clearly visible that the character of the ZTD time series from stations like CASC (Portugal), SFER (Spain), MAS1 (Spain), or CAGL (Italy) are affected by prevailing weather conditions which are typical for the neighborhood of warm water reservoirs. This is mainly reflected in the smallest annual oscillations in Europe (e.g. CASC 22.6 mm, SFER 24.2 mm) and the biggest mean ZTD values (e.g. CASC 2.425 m, SFER 2.423 m). RAMO (Israel) is also located near the Mediterranean coast. However, despite the proximity of warm water masses, it is characterized by much lower humidity and annual amplitudes (the annual amplitude at the RAMO station reaches 13.72 mm and the mean ZTD value is up to 2.153 m). This is due to the fact that this station is located at the altitude of 893.1 m above sea level, on the border of the Moderate Mediterranean and Dry Arid climate zones. In the central part of Europe it is possible to distinguish less (in the interior of the continent) and more (closer to the ocean) humid varieties of the temperate climate zone. Stations located within a humid variety usually have higher mean ZTD values and smaller annual amplitudes as compared to the stations situated in the interior of the continent. Stations like: HERS (United Kingdom) with 2.405 m of the ZTD mean and 41.0 mm of the annual amplitude or WARE (Belgium) with 2.374 m ofthe ZTD mean and 44.5 mm of the annual amplitude compared to the LAMA (Poland) with 2.358 m of the ZTD mean and 52.2 mm of the annual amplitude or PENC (Hungary) with 2.350 m of the ZTD mean and 52.9 mm of the annual amplitude could be a good example. Different characters of the ZTD time series from a few selected stations are presented in Fig. 4. Topography near the station should be taken into consideration in case of assigning features which are characteristic for selected climate zones to the ZTD time series. Mountain massifs that affect the formation of mountainous type of climate can be given as an example of such conditions. They can also disturb movements of air masses, thereby forming e.g. precipitation shadows.

5 Results of trend analysis

The trend values for 57 EPN stations were estimated using the LSE method, and in the next step their presence was confirmed using the Mann-Kendall trend test (in case of both reprocessing campaigns). Only the stations for which the trend was confirmed were used to determine the average trend for the whole Europe. In Repro 1, the occurrence of a trend was confirmed for 53 of 57 stations and four stations were rejected from the analysis: CASC (Portugal), MATE (Italy), MEDI (Italy) and TORI (Italy). For the remaining 53 stations the average value of the trend was equal to 1.0 mm/decade. 33 stations had positive trend characters and 20 stations had negative trend characters. In Repro2, the Mann-Kendall trend test gave the False results for 5 stations: GRAS (France), GRAZ (Austria), MATE (Italy), SFER (Spain) and TRO1 (Norway). For the remaining stations, the average trend value was 0.3 mm/decade, including 30 stations with positive and 22 stations with negative trend values. The

Atmos. Meas. Tech. Discuss., doi:10.5194/amt-2016-5, 2016
Manuscript under review for journal Atmos. Meas. Tech.
Published: 1 February 2016

Atmospheric Measurement Techniques Discussions

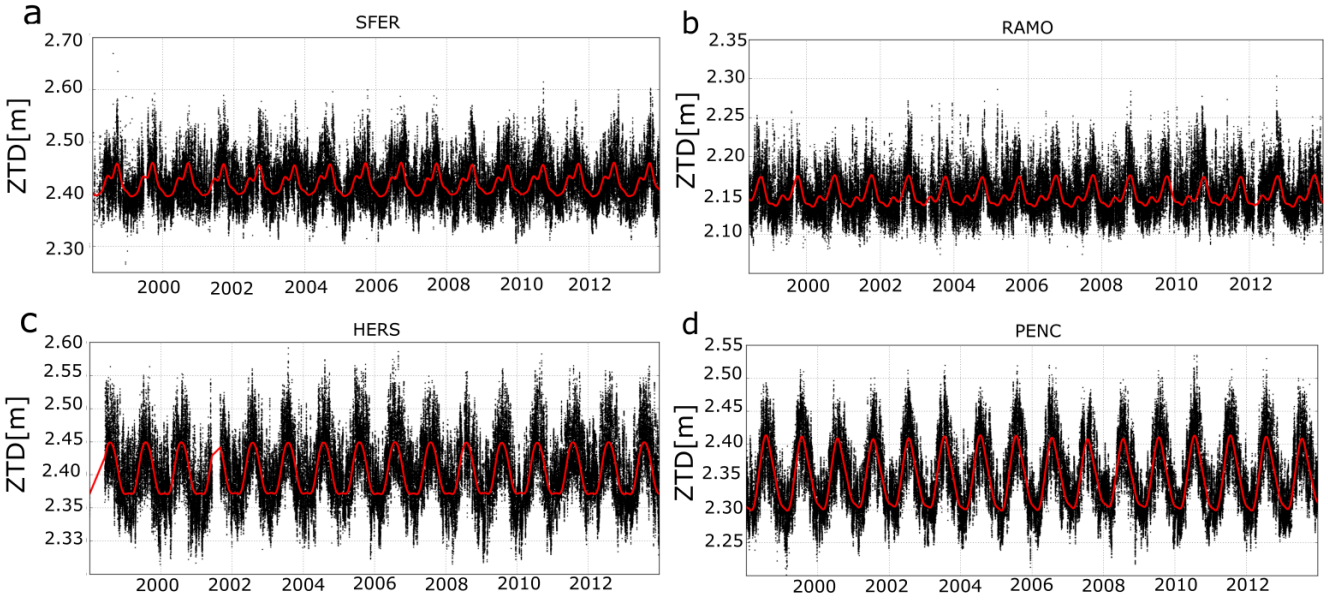

Figure 4. ZTD time series for SFER (a), RAMO (b), HERS (c), and PENC (d) stations with fitted oscillations.

highest positive trend in Repro1 was 5.5 mm/decade for BZRG (Italy), while in the Repro 2 campaign it was 5.8 mm/decade for GLSV (Ukraine). The highest negative trend value was found for the GOPE station (Czech Republic) both for the Repro1 and the Repro2 campaigns. However, in the first reprocessing campaign it was -4.7 mm/decade and in the second it was -7.1 mm/decade. Results for all stations included in the analysis are presented in Fig. 5. Stations with negative results of the Mann-Kendall trend test are indicated with a black dot. Distribution of the trend characters is similar in both cases. There are only discrepancies in the values of the negative trends. In Repro2 they are noticeably bigger than in Repro1 which is reflected in the average value of the trend for the whole Europe determined separately for both campaigns. The area of north-eastern and south-eastern Europe is characterized by positive trend values on both maps, with some discrepancies in the values. Similar consistency of the trends nature occurs in the area of western and south-western Germany, the Netherlands, Belgium and north-eastern France, where trends with only negative character occur in both the Repro 1 and the Repro2 campaigns. A clear coherence of trend characters for such large areas proves that they were not a result of random phenomena, but they rather followed consistent changes. The biggest inconsistency of the nature of the trend occurs in central and southern Europe. In this area, trends with opposite signs exist in close neighborhood (both in case of the Repro1 and the Repro2 campaigns). However, it is worth to notice that there is a large topographical variety (the presence of highlands and mountain ranges) which has a very large influence on movement of air masses and therefore on forming of prevailing weather conditions. The differences are observed both in the mean trend value of ZTD for the entire Europe (1.0 mm/decade in case of Repro1 and 0.3 mm/decade in case of Repro2) and in the maps presented in Fig. 5. To obtain more precise information about the extent of the differences for each station, the trend value derived from the first reprocessing was subtracted from the trend value obtained from the later

Atmos. Meas. Tech. Discuss., doi:10.5194/amt-2016-5, 2016
Manuscript under review for journal Atmos. Meas. Tech.
Published: 1 February 2016

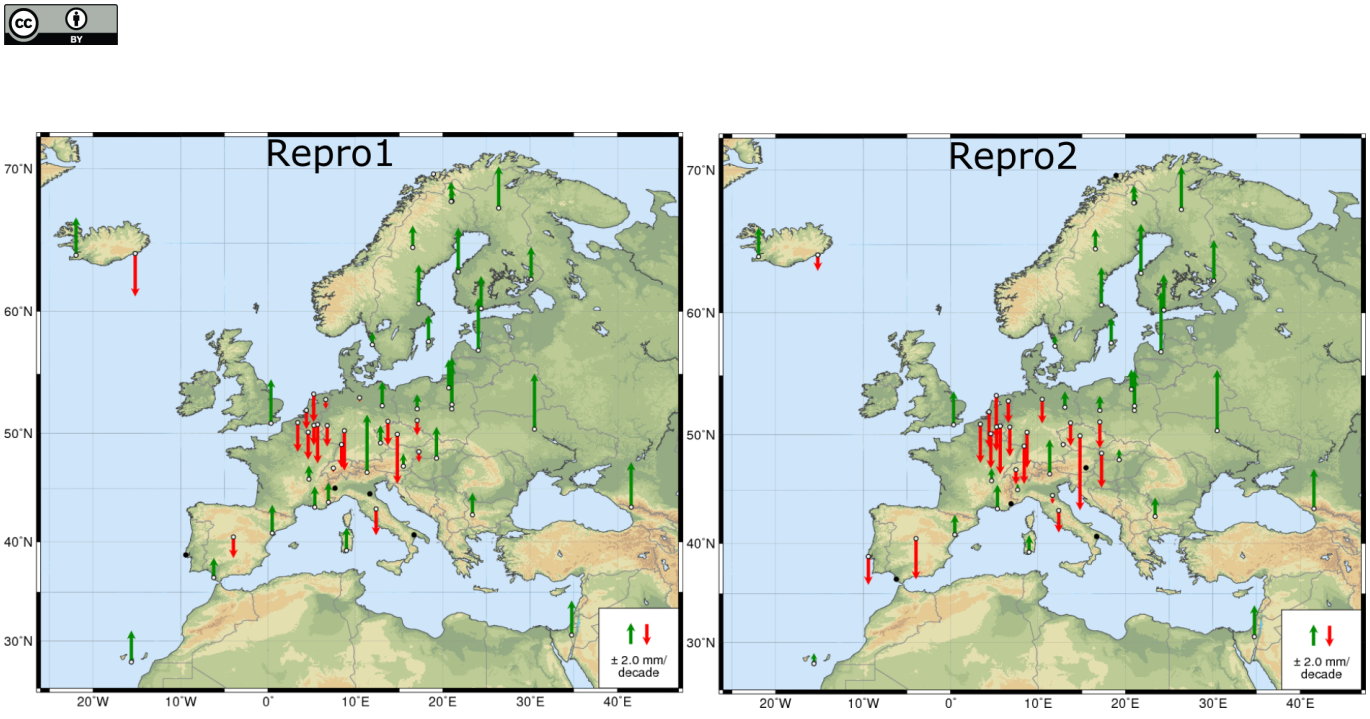

Figure 5. ZTD trend for 16-year time series (January of 1998 through December of 2013) obtained from the Repro1 campaign (left) and ZTD trend for 16-year time series (January of 1998 through December of 2013) obtained from the Repro2 campaign (right).

reprocessing. In Repro2, 43 stations had smaller trend value than in Repro1, 13 stations had higher values and only one station had exactly the same value of the trend (BOR1). The differences reach the value of 2.6 mm/decade. More details concerning the differences in the trend values between the Repro2 and the Repro1 campaigns are shown in Fig. 6. As it was mentioned above, the optimum spatial distribution was one of the factors in favor of shortening the time-series to the period of January of 1998 through December of 2013. However, in case of climate monitoring it is worth to work on the longest possible time series. Such data provide more reliable results, especially in case of investigating the presence and value of linear tends. Therefore, the following analysis was performed for 28 EPN station, which have been operated continuously since 1996. The adopted method of analysis was the same as in case of the shorter period.

In Repro1, the Mann-Kendall trend test gave negative results for 2 stations: DELF (Netherlands) and WARE (Belgium). For the rest of them, the mean value of the trend was 1.8 mm/decade, including 5 stations with negative and 21 with positive character of the trend. The highest positive trend value of 5.0 mm/decade was found for the RIGA station (Latvia). The highest negative trend value of -4.1 mm/decade was found (as in the case of the 16-year ZTD time series) for the GOPE station (Czech Republic). In Repro2, negative results of the Mann-Kendall trend test had six stations: GRAS (France), MATE (Italy), MEDI (Italy), SFER (Spain), WARE (Belgium) and ZIMM (Switzerland). The mean value of the trend for the remaining 22 stations was 1.0 mm/decade. The highest positive trend value occurred in RIGA (Latvia), however, it was higher than in the case of Repro1 and reached 5.7 mm/decade. As previously in Repro1, GOPE (Czech Republic) had the highest negative trend value, though different (-7.1 mm/decade). Spatial distribution of trends (and their characters) for Repro1 and Repro2 are presented in Fig. 7. These maps clearly show why the mean value of trends in case of the 18-year ZTD time series is higher than in case

Atmos. Meas. Tech. Discuss., doi:10.5194/amt-2016-5, 2016
Manuscript under review for journal Atmos. Meas. Tech.
Published: 1 February 2016

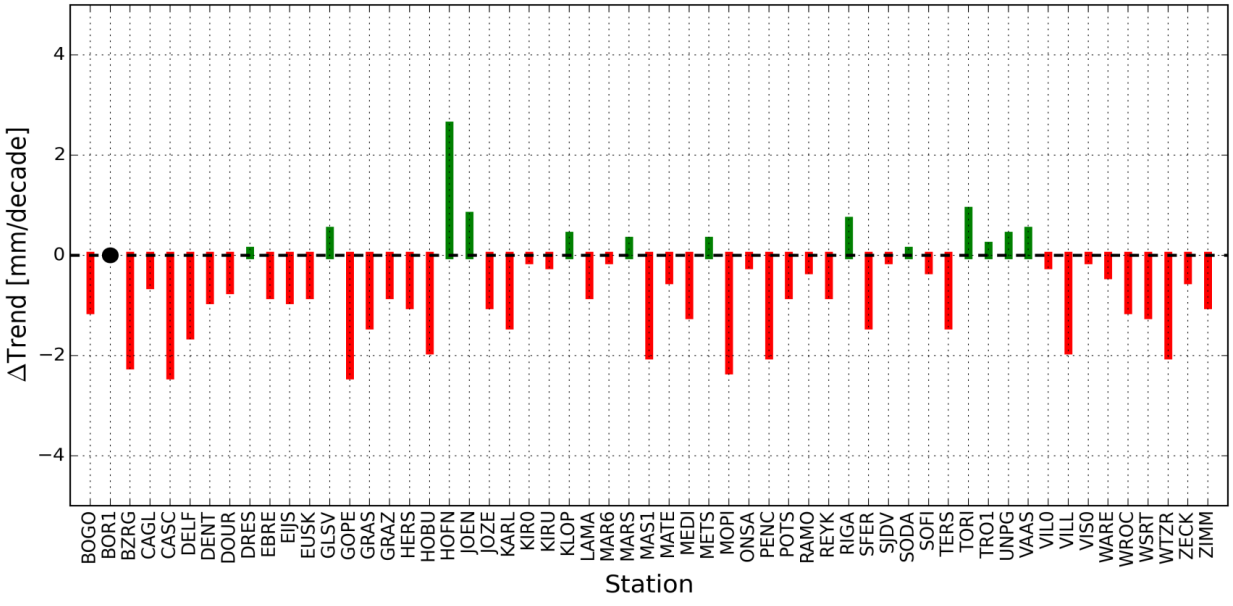

Figure 6. Differences between the values of the 16-year linear trends obtained from the Repro2 and the Repro1 campaigns.

of the 16-year ZTD time series. This is because most stations with negative trends (which occurred especially in the area of western and south-western Germany, the Netherlands, Belgium and north-eastern France) were not included in this analysis (too short time series). This resulted in greater consistency and homogeneity in the estimated ZTD trends because most stations which were included in the 18-year ZTD analysis had positive trends characters. Moreover, in Repro1, the number of stations for which the Mann-Kendal trend test gave negative results (only 2 stations) decreased for the longer period. In Repro2 six stations had negative results of the Mann-Kendall trend test. Therefore, the spatial distribution of stations in Repro2 looks poorer than in Repro1. It is also worth to notice that for the 18-year period the Mann-Kendall trend test gave negative results for different stations than for the shorter period. This is particularly noticeable for results based on the data from the Repro1 campaign where none station had the same result of the Mann-Kendall trend test. At the same time, in Repro2 there were only two such stations: GRAS (France) and MATE (Spain). However, in both cases in central and southern Europe the negative trend areas occurred next to the positive ones which is consistent with the results obtained from analysis of the 16-year ZTD time series. Similar consistency of the results can also be seen in the area of north-eastern Europe where only positive trends occurred. Finally, trends obtained from Repro2 were smaller than those from the Repro1 campaign, regardless of the length of the analyzed period of time. As in the case of the 16-year time series analysis, there were differences between results based on different GPS processing strategies (between both campaigns). To obtain information about the extent of the differences in the trend values for each station, the trend value derived from Repro1 was subtracted from the trend value obtained from the second campaign. Similarly as in the previous analysis, the results based on Repro2 were generally lower than the results from Repro1. In more detail: 24 stations had lower value of the linear trend, 2 stations had it higher and only 2 stations had exactly

Atmos. Meas. Tech. Discuss., doi:10.5194/amt-2016-5, 2016
Manuscript under review for journal Atmos. Meas. Tech.
Published: 1 February 2016

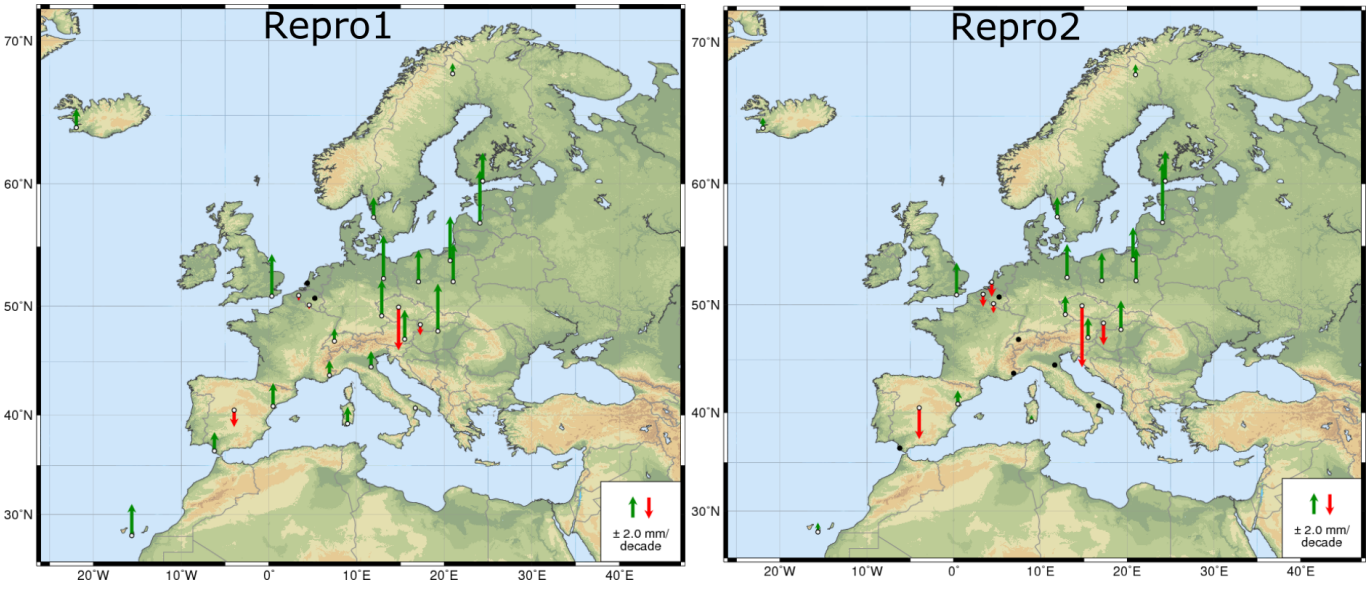

Figure 7. ZTD trend for the 18-year time series (January of 1996 through December of 2013) obtained from the Repro1 campaign (left) and ZTD trend for the 18-year time series (January of 1996 through December of 2013) obtained from the Repro2 campaign (right).

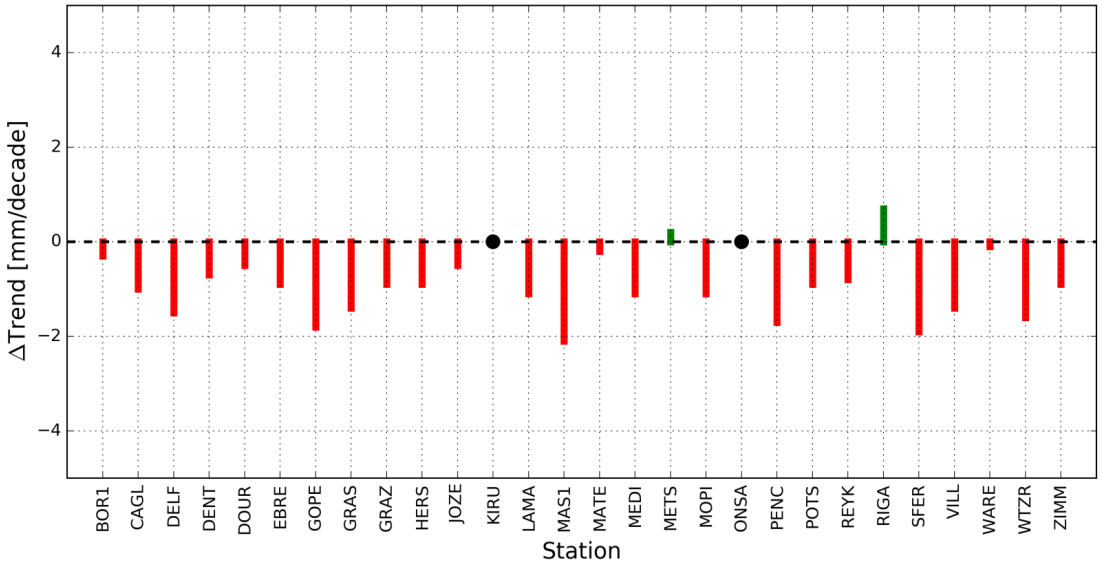

Figure 8. Differences between the values of the 18-year linear trends obtained from the Repro2 and the Repro1 campaigns.

the same trend value (KIRU and ONSA). The details of the differences between both reprocessing campaigns are shown in Fig. 8. Differences in the number of stations for which the trend is confirmed (for both lengths of the time series) and differences

Atmos. Meas. Tech. Discuss., doi:10.5194/amt-2016-5, 2016
Manuscript under review for journal Atmos. Meas. Tech.
Published: 1 February 2016

Atmospheric Measurement Techniques Discussions

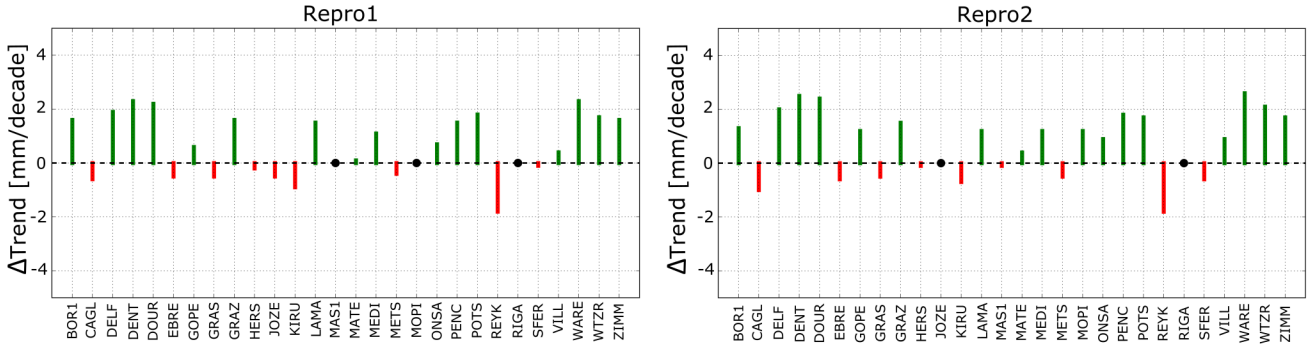

Figure 9. Differences in trend values for the 18-year and the 16-year time series obtained from the Repro1 (left) and Repro2 (right) campaign.

in the ZTD trend values confirm that it is necessary to work on exactly the same period of time to analyze the changes of the spatial distribution of the ZTD trends. Two additional years in the length of the time series may be important not only for the estimated value of the trend but also for its character. The ZIMM station (Switzerland) is an example of such change. In both reprocessing campaigns it had a negative character for the shorter period and a positive one for the longer period. The values of the trends were not significant: -0.4 mm/decade for the 16-year and 1.4 mm/decade for the 18-year in the Repro1 campaign, and -1.4 mm/decade for the 16-year and 0.3 mm/decade for the 18-year time series in the Repro2 campaign. However, it is worth to notice, that the characters were the same for various GPS processing strategies. This confirms that the change of the values of the linear trend was not accidental. Moreover, both in Repro1 and Repro2, the values of the trends for the longer periods were generally bigger than for the shorter periods. It should also be emphasized that the values of the differences between the two periods were at the same level and they had the same characters, both for Repro1 and Repro2 which is shown in Fig. 9.

6 Discussion

Generally, the trend values in Repro2 were smaller (for both lengths of the time series) than in Repro1. In view of the fact that in both reprocessing campaigns the same raw data were used, the differences had to have their source in the processing strategy. The impact of the adopted elevation mask on the long time series was discussed inter alia by Ning and Elgered (Ning and Elgered, 2012). Having analyzed GPS and VLBI data they indicated that the best consistency in IWV trends between these two techniques is achieved for 25° elevation mask. Tregoning and Herring (Tregoning and Herring, 2006) presented that a priori ZHD value had influence on both coordinates (vertical) and the ZTD value. The studies were not, however, related to the long term dependence, especially with taking into account climate applications. To assess the possible impact of the mapping function on long time changes of the ZTD parameter, the authors selected 28 stations. The analysis of ZHD (which is responsible for about 90% of the total value of the delay) long term variability was conducted for all of them. The ZHD value was taken from the same source as in case of the second reprocessing campaign in which a priori value of ZHD was derived from VMF1. The authors focused on this data source because NMF, which was used in Repro1, provides data which

Atmos. Meas. Tech. Discuss., doi:10.5194/amt-2016-5, 2016
Manuscript under review for journal Atmos. Meas. Tech.
Published: 1 February 2016

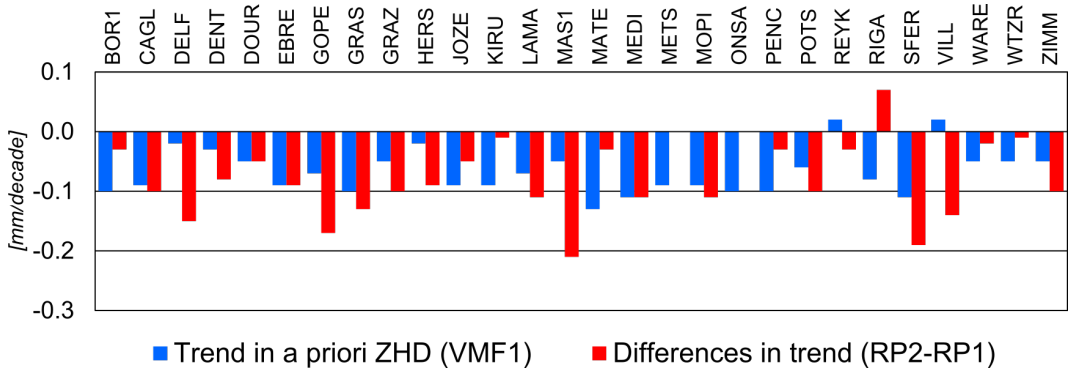

Figure 10. Differences in trend values for the 18-year and the 16-year time series obtained from the Repro2 campaign.

depends only on the day of the year, latitude and altitude above sea level. Therefore, they could not have time dependence over time scales of many years. The mean trend value of ZHD from VMF1, for all 28 selected stations, was -0.7 mm/decade, while the mean difference in ZTD trend value between Repro2 and Repro1 (for the same stations) was -0.8 mm/decade. Of course, at this stage it cannot be clearly said that the adopted a priori ZHD value could have such a big influence on the ZTD trend value. However, it is worth to notice that the negative trend value of the ZHD VMF generally matches the smaller value of the ZTD trends obtained from the Repro2 campaign. There was only 0.1 mm/decade difference between the ZHD VMF1 mean trend value and the differences: Repro2 - Repro1. Nevertheless, this similarity does not completely solve the problem of the discrepancies in trends. A detailed analysis for individual stations showed in fact, that for individual stations the trend value in the adopted a priori ZHD data was not equal to the differences: Repro2 – Repro1. For most stations, these two parameters have similar character, and for some of them even the value. For some stations, such as DELF (Netherlands), MAS1 (Spain), METS (Finland), ONSA (Sweden), RIGA (Latvia) or VILL (Spain) the adopted a priori ZHD cannot explain the differences of the trend value between the Repro2 and the Repro1 campaigns (see Fig. 10). Besides the differences of trend values between Repro2 and Repro1, it is worth to notice that both reprocessing campaigns gave almost the same results for differences between the longer and the shorter periods of time (Fig. 11). This means, that the adopted processing strategy did not directly influence the detected changes caused by the additional two years. Therefore, it could be indicated that the effect of non-linear changes in the state of the troposphere (caused by weather conditions which occurred during the additional period of time) had the same impact on the trend value, regardless of the method of ZTD estimation.

7 Summary and conclusions

The ZTD time series obtained from two different reprocessing campaigns were analyzed in this paper. The purpose of this work was to assess differences in data between the two sources, especially taking into consideration their usefulness for climate studies. In the first step, the process of screening was conducted to obtain the most homogeneous data sets. Information about various types of oscillations was obtained from the Lomb-Scargle periodograms which were prepared for every station.

Atmos. Meas. Tech. Discuss., doi:10.5194/amt-2016-5, 2016
Manuscript under review for journal Atmos. Meas. Tech.
Published: 1 February 2016

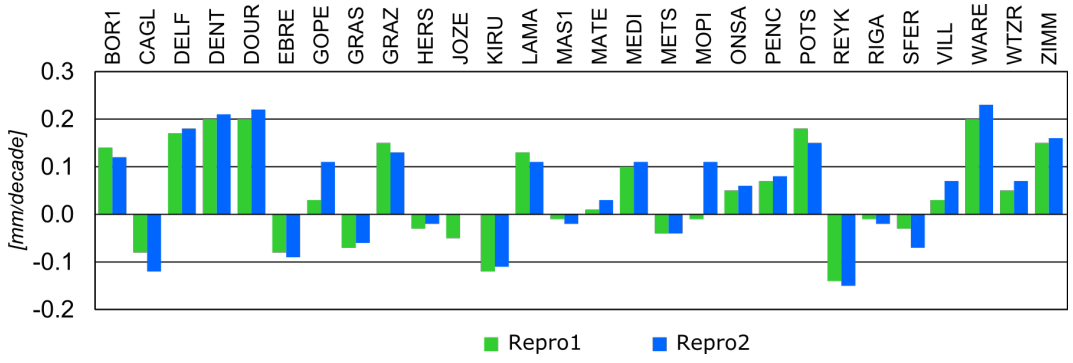

Figure 11. Differences of the trend value between the 18-year and the 16-year time series, for the Repro1 (green) and the Repro2 (blue) campaigns.

Then, the value of the seasonal components and the linear trends were estimated using the Least Square Estimation method. Finally, the Mann-Kendall trend test was performed to confirm the presence of a trend in the ZTD time series. On the one hand, the spectral analysis showed that differences in the amplitude and phase of the annual period are almost identical in both campaigns (usually below 1.0 mm). Especially, when compared to the mean value of the amplitude, which was about 46 mm, the differences seem insignificant. The highest and lowest annual amplitudes were found for the TORI station, it was even exactly the same in Repro1 and Repro2 (63.3 mm). The differences between the seasonal components are so small that it can be concluded that the processing strategy does not significantly affect them. Consequently, it can be stated that they can be used as a reliable source of data for climate studies. Seasonal oscillations reflect prevailing weather conditions which occur in a given region. Their values reflect the strength of the annual changes in weather, including increasing or decreasing influence of warm water masses, atmospheric pressure centers or other factors affecting the formation of weather. In this sense, due to high spatial resolution, the GPS observations can bring significant benefits to the climate community. On the other hand, long-term changes of ZTD are not so clear. The linear trend in the ZTD time series is particularly important for the purposes of climate studies, because it reflects the increase or decrease of temperature or water vapor content in the atmosphere. The existence of a linear trend in the ZTD time series demonstrates therefore that some physical and real changes take place in the troposphere. Hence, regardless of the selected techniques, its value should be similar or identical. Despite this, the occurrence of differences in the tropospheric parameters values between the various techniques is well known, as they are based on different measurement mechanisms. In case of the GPS technique and this study, we are dealing with the use of exactly the same measurement equipment (receivers and antennas). Therefore, the obtained differences could be only caused by the applied processing strategies. In this paper, the linear trend was considered in two lengths of the time series: 16-year and 18-year, for both reprocessing campaigns. For the shorter period, the station with the highest positive trend value was not the same for the two sets of data. In Repro1 it was BZRG (Italy), for which the trend was 5.5 mm/decade, while in Repro2 it was GLSV (Ukraine) with 5.8 mm/decade. In contrast, GOPE (Czech Republic), was the station with the highest negative trend value in both campaigns. However, the trend values were significantly different: -4.7 mm/decade (Repro1) and

Atmos. Meas. Tech. Discuss., doi:10.5194/amt-2016-5, 2016
Manuscript under review for journal Atmos. Meas. Tech.
Published: 1 February 2016

-7.1 mm/decade (Repro2). Different trends were also obtained for the longer 18-year ZTD time series. In this case, the station with the highest positive trend value was RIGA (Latvia) in both campaigns, but the trend values were significantly different: 5.0 mm/decade and 5.7 mm/decade for Repro1 and Repro2, respectively. Again, the highest negative trend values were found for GOPE: -4.1 mm/decade and -5.9 mm/decade for Repro1 and Repro2, respectively. Generally, the trends in Repro2 were smaller in comparison to Repro1. In case of the shorter period, the mean trend value in Repro2 was 0.7 mm/decade smaller than in Repro1. Similarly, in case of the longer period the difference was 0.8 mm/decade. At the same time, the differences between the 18-year and the 16-year ZTD time series were similar in both campaigns. This proves that changing the length of the analyzed time series influences in the same way, independently of the data sources. The obtained results indicated that the linear changes of ZTD seem to be more sensitive to the applied processing strategy than the seasonal components. The method used for the trend estimation was exactly the same for both campaigns, so the differences in its values resulted only from different approaches to ZTD determination. Investigation of factors which have the biggest influence on the differences is very important in further interpretations. Awareness of the limitations and error sources of ZTD derived from GPS observations, may improve the reliability of the IWV conversion results. Differences in the ZTD values presented in this paper could result from application of various mapping functions which are based on various sources of meteorological data (the Niell Mapping Functions are based on radiosonde profiles and the Vienna Mapping Functions 1 are based on the ECMWF weather model). The differences could also be affected by the sequence of determination of the final ZTD value. In Repro1, ZTD was fixed to weekly coordinates, while in Repro2 it was estimated together with the other parameters, including coordinates, in daily solutions. Finally, application of atmospheric loadings in Repro2, which have direct impact on the estimated height, could also affect the estimated ZTD. However, it is hard to explicitly separate the influence of each parameter using only the compared data sets and further analyses are still needed. Nevertheless, the results clearly show that GPS may be a promising source of data for climate studies.

Appendix A: Detailed results of analysis

Acknowledgements. This research was financed with statutory research funds by the Faculty of Civil Engineering and Geodesy of the Military University of Technology.

The authors would also like to acknowledge the contribution of the COST Action ES1206

Atmos. Meas. Tech. Discuss., doi:10.5194/amt-2016-5, 2016
Manuscript under review for journal Atmos. Meas. Tech.
Published: 1 February 2016

References

Baldysz, Z., Nykiel, G., Araszkiewicz, A., Figurski, M., and szafranek, K.: Investigation of the 16-year and 18-year ZTD Time Series Derived from GPS Data Processing, Acta Geophysica, 63, doi:10.1515/acgeo-2015-0033, 2015.

Bengtsson, L., Hagemann, C., and Hodges, K.: Can climate trends be calculated from reanalysis data?, Journal of Geophysical Research, 109, doi:10.10+/2004JD004536, 2004.

Bevis, M., Businger, S., Herring, T., Rocken, C., Anthes, R., and Ware, R.: GPS meteorology: Remote sensing of atmospheric water vapor using the global positioning system, Journal of Geophysical Research, 97, doi:10.1029/92JD01517, 1992.

Bock, O., Bouin, M., Walpersdorf, A., Lafore, J., Janicot, S., Guichard, F., and Agusti-Panareda, A.: Comparison of ground-based GPS precipitable water vapour to independent observations and numerical weather prediction model reanalyses over Africa, Quarterly Journal of the Royal Meteorological Society, 133, doi:10.1002/qj.185, 2007.

Bock, O., Willis, P., Wang, J., and Mears, C.: A high-quality, homogenized, global, long-term (1993–2008) DORIS precipitable water data set for climate monitoring and model verification, Journal of Geophysical Research Atmospheres, 119, doi:10.1002/2013JD021124, 2014.

Boehm, J., Werl, B., and Schuh, H.: Troposphere mapping functions for GPS and very long baseline interferometry from European Centre for Medium-Range Weather Forecasts operational analysis data, Journal of Geophysical Research, 111, doi:10.1029/2005JB003629, 2006.

Bruyninx, C.: The EUREF Permanent Network: a multi-disciplinary network serving surveyors as well as scientists, GeoInformatics, 7, 2004.

COST: Memorandum of Understanding For the implementation of a European Concerted Research Action designated as: COST Action ES1206 Advanced Global Navigation Satellite Systems Tropospheric Products for monitoring Severe Weather Events and Climate (GNSS4SWEC), in: COST Action ES1206, 2012.

Dach, R., Hugentobler, U., Fridez, P., and Meindl, M.: Bernese GPS Software Version 5.0, Journal of Geophysical Research Atmospheres, 119, doi:10.1002/2013JD021124, 2014.

Davis, J., Herring, T., Shapiro, I., Rogers, E., and Elgered, G.: Geodesy by radio interferometry: Effects of atmospheric modeling errors on estimates of baseline length, Radio Science, 20, doi:10.1029/RS020i006p01593, 1985.

Elósegui, P., Davis, J., Jaldehag, R., Johansson, J., Niell, A., and Shapiro, I.: Geodesy using the global positioning system: The effects of signal scattering on estimates of site position, Journal of Geophysical Research, 100, doi:10.1029/95JB00868, 1995.

Emardson, T., Elgered, G., and Johansson, J.: Three months of continuous monitoring of atmospheric water vapour with a network of Global Positioning System receivers, Journal of Geophysical Research, 103, doi:10.1029/97JD03015, 1998.

Figurski, M., Kamiński, P., and Kenyeres, A.: Preliminary results of the complete EPN reprocessing computed by the MUT EPN Local Analysis Centre, Bulletin of Geodesy and Geomatics, 1/2009, 2009.

Guerova, G.: Ground based GNSS Meteorology, in: Gfg Summer School, 2013.

Hagemann, S., Bengtsson, L., and Gendt, G.: On the determination of atmospheric water vapor from GPS measurements, Journal of Geophysical Research, 108, doi:10.1029/2002JD003235, 1992.

Herring, T.: Modelling atmospheric delays in the analysis of space geodetic data, in: de Munck JC, Spoelstra TAT (eds) Proceedings of the symposium refraction of transatmospheric signals in geodesy, 1992.

Jin, S., Park, J., Cho, J., and Park, C.: Seasonal variability of GPS-derived zenith tropospheric delay (1994–2006) and climate implications, Journal of Geophysical Research, 112, doi:10.1029/2006JD007772, 2007.

Kendall, M. and Stuart, A.: The Advanced Theory of Statistics, The Annals of Mathematical Statistics, 19, doi:10.1017/S0020269X00008276, 1970.

King, R., Herring, T., and Mccluscy, S.: Documentation for the GAMIT GPS analysis software 10.4., Tech. rep., Massachusetts Institute of Technology, 2010.

Lomb, N.: Least-squares frequency analysis of unequally spaced data, Astrophysics and Space Science, 39, doi:10.1007/BF00648343, 1976.

Mann, H.: Nonparametric Tests Against Trend, Econometrica, 13, doi:10.2307/1907187, 1945.

Marini, J.: Correction of satellite tracking data for an arbitrary tropospheric profile, Radio Science, 7, doi:10.1029/RS007i002p00223, 1972.

Niell, A.: Global mapping functions for the atmospheric delay at radio wavelengths, Journal of Geophysical Research, 101, doi:10.1029/95JB03048, 1996.

Nilsson, T. and Elgered, G.: Long-term trends in the atmospheric water vapor content estimated from ground-based GPS data, Journal of Geophysical Research, 113, doi:10.1029/2008JD010110, 2008.

Ning, T. and Elgered, G.: Trends in Atmopsheric Water Vapour Content From Ground-Based GPS: The Impact of the Elevation Cutoff Angle, IEEE Journal of Selected Topics in Applied Earth Observations and Remote Sensing, 5, doi:10.1109/JSTARS.2012.2191392, 2012.

Pacione, R., Pace, B., and Bianco, G.: An homogeneously reprocessed Zenith Total Delay long-term time series over Europe, in: EGU General Assembly, 2014.

Petrie, E., King, M., Moore, P., and Lavallee, D.: Higher-order ionospheric effects on the GPS reference frame and velocities, Journal of Geophysical Research, 115, doi:10.1029/2009JB006677, 2010.

Schmid, R., Steigenberger, P., Gendt, G., Ge, M., and Rothacher, M.: Generation of a consistent absolute phase center correction model for GPS receiver and satellite antennas, Journal of Geodesy, 81, doi:10.1007/s00190-007-0148-y, 2007.

Soden, B. and Held, I.: Robust responses of the hydrological cycle to global warming, Journal of Climate, 19, doi:10.1175/JCLI3990.1, 2006.

Sohne, W., Figurski, M., and Szafranek, K.: Homogeneous Total Zenith Delay Parameter Estimation from European Permanent GNSS sites, Bulletin of Geodesy and Geomatics, 69, 2010.

Stoew, B., Nilsson, T., Elgered, G., and Jarlemark, P.: Temporal correlations of atmospheric mapping function errors in GPS estimation, Journal of Geodesy, 81, doi:10.1007/s00190- 006-0114-0, 2007.

Tesmer, V., Boehm, J., Heinkelmann, R., and Schuh, H.: Effect of different tropospheric mapping functions on the TRF, CRF and position time-series estimated from VLBI, Journal of Geodesy, 81, doi:10.1007/s00190-006-0126-9, 2007.

Tregoning, P. and Herring, T.: Impact of a priori zenith hydrostatic delay errors on GPS estimates of station heights and zenith total delays, Geophysical Research Letters, 33, doi:10.1029/2006GL027706, 2006.

Van Malderen, R., Brenot, H., Pottiaux, E., Hermans, C., De Mazierre, M., Wagner, T., De Becker, H., and Bruyninx, C.: A multi-site intercomparison of integrated water vapour observations for climate change analysis, Atmospheric Measurement Techniques, 7, doi:10.5194/amt-7-2487-2014, 2014.

Vey, S., Dietrich, R., Fritsche, M., Rülke, M., Rothacher, M., and Steigenberger, P.: Influence of mapping function parameters on global GPS network analyses: Comparisons between NMF and IMF, Geophysical Research Letters, 33, doi:10.1029/2005GL024361, 2006.

Wang, J. and Zhang, L.: Climate applications of a global, 2-hourly atmospheric precipitable water dataset derived from IGS tropospheric products, Journal of Geodesy, 83, doi:10.1007/s00190-008-0238-5, 2009.

Wilgan, K., Rohm, W., and Bosy, J.: Multi-observation meteorological and GNSS data comparison with Numerical Weather Prediction model, Atmospheric Research, 156, doi:10.1016/j.atmosres.2014.12.011, 2014.

Atmos. Meas. Tech. Discuss., doi:10.5194/amt-2016-5, 2016
Manuscript under review for journal Atmos. Meas. Tech.
Published: 1 February 2016

Atmospheric Measurement Techniques Discussions

Yong, W., Binyun, Y., Debao, W., and Yanping, L.: Zenith Tropospheric Delay from GPS monitoring climate change of Chinese Mainland, Education Technology and Training, 2008. and 2008 International Workshop on Geoscience and Remote Sensing. ETT and GRS 2008. International Workshop on, 1, doi:10.1109/ETTandGRS.2008.43, 2008.

Atmos. Meas. Tech. Discuss., doi:10.5194/amt-2016-5, 2016
Manuscript under review for journal Atmos. Meas. Tech.
Published: 1 February 2016

Atmospheric Measurement Techniques Discussions

Table 2. Results of analysis of the 16 year ZTD time series from the first (Repro1) and the second (Repro2) EPN reprocessing campaigns

Station	Annual amplitude (mm)	Semiannual amplitude (mm)	Trend value (mm/decade)	ZTD Mean (m)	Annual amplitude (mm)	Semiannual amplitude (mm)	Trend value (mm/decade)	ZTD Mean (m)
	Repro1				**Repro2**			
BOGO	52.79 ± 0.19	9.44 ± 0.18	0.47 ± 0.02	2.374	52.50 ± 0.19	9.50 ± 0.19	0.35 ± 0.02	2.375
BOR1	52.00 ± 0.18	9.40 ± 0.18	0.16 ± 0.02	2.385	51.51 ± 0.19	9.52 ± 0.19	0.15 ± 0.02	2.386
BZRG	61.92 ± 0.19	6.37 ± 0.18	0.55 ± 0.02	2.347	61.75 ± 0.19	6.62 ± 0.19	0.33 ± 0.02	2.348
CAGL	37.60 ± 0.18	3.42 ± 0.18	0.22 ± 0.02	2.376	37.30 ± 0.18	3.08 ± 0.18	0.16 ± 0.02	2.376
CASC	22.48 ± 0.22	1.69 ± 0.21	-0.04 ± 0.02	2.425	22.30 ± 0.22	1.39 ± 0.21	-0.28 ± 0.02	2.427
DELF	44.08 ± 0.19	7.92 ± 0.19	-0.16 ± 0.02	2.405	42.95 ± 0.20	8.33 ± 0.20	-0.32 ± 0.02	2.405
DENT	44.12 ± 0.20	7.63 ± 0.20	-0.25 ± 0.02	2.412	43.26 ± 0.20	8.01 ± 0.20	-0.34 ± 0.02	2.413
DOUR	44.01 ± 0.19	7.67 ± 0.19	-0.25 ± 0.02	2.346	43.36 ± 0.19	8.06 ± 0.19	-0.32 ± 0.02	2.347
DRES	50.96 ± 0.18	8.41 ± 0.18	-0.22 ± 0.02	2.370	50.80 ± 0.19	8.79 ± 0.19	-0.21 ± 0.02	2.370
EBRE	54.32 ± 0.21	8.92 ± 0.21	0.29 ± 0.02	2.425	53.85 ± 0.21	9.19 ± 0.21	0.21 ± 0.02	2.426
EIJS	46.14 ± 0.19	8.10 ± 0.19	-0.34 ± 0.02	2.402	45.44 ± 0.20	8.40 ± 0.20	-0.44 ± 0.02	2.402
EUSK	46.39 ± 0.19	7.91 ± 0.19	-0.19 ± 0.02	2.358	45.59 ± 0.19	8.08 ± 0.19	-0.28 ± 0.02	2.359
GLSV	53.38 ± 0.17	10.59 ± 0.17	0.53 ± 0.02	2.352	53.42 ± 0.17	10.64 ± 0.17	0.58 ± 0.02	2.352
GOPE	48.81 ± 0.17	8.40 ± 0.17	-0.45 ± 0.02	2.255	48.81 ± 0.17	8.54 ± 0.17	-0.70 ± 0.02	2.256
GRAS	41.75 ± 0.17	2.46 ± 0.17	0.19 ± 0.02	2.055	41.58 ± 0.17	2.79 ± 0.17	0.05 ± 0.02	2.056
GRAZ	56.30 ± 0.16	8.06 ± 0.16	0.12 ± 0.02	2.281	56.18 ± 0.16	8.28 ± 0.16	0.04 ± 0.02	2.281
HERS	41.00 ± 0.21	7.86 ± 0.21	0.42 ± 0.02	2.406	40.09 ± 0.21	8.22 ± 0.21	0.32 ± 0.02	2.407
HOBU	47.22 ± 0.19	8.10 ± 0.19	-0.03 ± 0.02	2.377	46.39 ± 0.19	8.32 ± 0.19	-0.22 ± 0.02	2.378
HOFN	42.62 ± 0.21	6.66 ± 0.21	-0.39 ± 0.02	2.360	41.35 ± 0.22	7.19 ± 0.22	-0.13 ± 0.02	2.360
JOEN	53.71 ± 0.19	11.89 ± 0.19	0.33 ± 0.02	2.349	53.64 ± 0.20	12.06 ± 0.20	0.41 ± 0.02	2.350
JOZE	52.96 ± 0.19	10.47 ± 0.18	0.41 ± 0.02	2.380	52.80 ± 0.19	10.17 ± 0.19	0.31 ± 0.02	2.379
KARL	49.68 ± 0.18	8.42 ± 0.18	-0.20 ± 0.02	2.386	49.07 ± 0.19	8.66 ± 0.19	-0.35 ± 0.02	2.387
KIR0	49.68 ± 0.17	9.43 ± 0.17	0.15 ± 0.02	2.224	49.26 ± 0.18	9.96 ± 0.18	0.14 ± 0.02	2.225
KIRU	50.52 ± 0.18	10.03 ± 0.18	0.22 ± 0.02	2.253	50.31 ± 0.19	10.57 ± 0.18	0.20 ± 0.02	2.254
KLOP	47.37 ± 0.19	7.82 ± 0.19	-0.36 ± 0.02	2.367	46.85 ± 0.19	8.10 ± 0.19	-0.32 ± 0.02	2.370
LAMA	52.36 ± 0.18	9.70 ± 0.18	0.29 ± 0.02	2.359	52.05 ± 0.19	9.77 ± 0.19	0.20 ± 0.02	2.359
MAR6	50.83 ± 0.19	9.32 ± 0.19	0.40 ± 0.02	2.370	50.28 ± 0.20	9.61 ± 0.20	0.39 ± 0.02	2.372
MARS	44.23 ± 0.22	1.22 ± 0.22	0.20 ± 0.02	2.419	44.31 ± 0.22	1.41 ± 0.22	0.22 ± 0.02	2.422
MAS1	29.97 ± 0.18	7.91 ± 0.18	0.30 ± 0.02	2.392	30.09 ± 0.18	7.47 ± 0.18	0.10 ± 0.02	2.394
MATE	40.90 ± 0.17	0.55 ± 0.16	0.01 ± 0.02	2.283	40.87 ± 0.17	0.29 ± 0.16	-0.04 ± 0.02	2.283
MEDI	54.35 ± 0.19	3.54 ± 0.19	0.04 ± 0.02	2.430	54.13 ± 0.19	3.79 ± 0.19	-0.08 ± 0.02	2.432
METS	50.68 ± 0.19	9.12 ± 0.19	0.35 ± 0.02	2.360	50.44 ± 0.20	9.31 ± 0.20	0.38 ± 0.02	2.362

Atmos. Meas. Tech. Discuss., doi:10.5194/amt-2016-5, 2016
Manuscript under review for journal Atmos. Meas. Tech.
Published: 1 February 2016

Atmospheric Measurement Techniques Discussions

Station	Annual amplitude (mm)	Semiannual amplitude (mm)	Trend value (mm/decade)	ZTD Mean (m)	Annual amplitude (mm)	Semiannual amplitude (mm)	Trend value (mm/decade)	ZTD Mean (m)
	Repro1				**Repro2**			
MOPI	49.97 ± 0.16	8.48 ± 0.16	-0.09 ± 0.02	2.256	50.62 ± 0.17	8.53 ± 0.17	-0.32 ± 0.02	2.262
ONSA	46.89 ± 0.19	8.33 ± 0.19	0.14 ± 0.02	2.390	46.35 ± 0.20	8.70 ± 0.20	0.13 ± 0.02	2.392
PENC	52.84 ± 0.17	8.38 ± 0.17	0.31 ± 0.02	2.351	52.88 ± 0.17	8.46 ± 0.17	0.11 ± 0.02	2.351
POTS	49.22 ± 0.18	8.59 ± 0.18	0.23 ± 0.02	2.378	48.49 ± 0.19	8.72 ± 0.19	0.16 ± 0.02	2.380
RAMO	13.80 ± 0.13	8.47 ± 0.13	0.34 ± 0.01	2.153	14.13 ± 0.13	8.26 ± 0.13	0.31 ± 0.01	2.154
REYK	42.68 ± 0.22	7.00 ± 0.22	0.39 ± 0.02	2.352	41.56 ± 0.23	7.53 ± 0.22	0.31 ± 0.02	2.353
RIGA	53.02 ± 0.19	9.98 ± 0.19	0.52 ± 0.02	2.391	52.92 ± 0.19	10.09 ± 0.19	0.60 ± 0.02	2.392
SFER	24.36 ± 0.20	4.59 ± 0.20	0.20 ± 0.02	2.423	24.27 ± 0.20	4.41 ± 0.20	0.05 ± 0.02	2.424
SJDV	45.63 ± 0.19	6.46 ± 0.19	0.13 ± 0.02	2.313	45.43 ± 0.20	6.75 ± 0.19	0.11 ± 0.02	2.315
SODA	51.21 ± 0.19	10.50 ± 0.19	0.42 ± 0.02	2.283	51.03 ± 0.19	10.94 ± 0.19	0.43 ± 0.02	2.284
SOFI	45.93 ± 0.15	3.74 ± 0.15	0.22 ± 0.02	2.118	45.76 ± 0.15	3.80 ± 0.15	0.18 ± 0.02	2.119
TERS	43.94 ± 0.19	8.20 ± 0.19	-0.25 ± 0.02	2.162	42.67 ± 0.20	8.50 ± 0.20	-0.39 ± 0.02	2.404
TORI	63.31 ± 0.21	5.95 ± 0.22	-0.03 ± 0.02	2.404	63.34 ± 0.21	6.36 ± 0.21	0.06 ± 0.02	2.355
TRO1	49.64 ± 0.18	8.83 ± 0.18	0.02 ± 0.02	2.354	49.09 ± 0.19	9.46 ± 0.19	0.05 ± 0.02	2.329
UNPG	46.69 ± 0.18	1.47 ± 0.18	-0.25 ± 0.02	2.328	46.36 ± 0.18	1.64 ± 0.18	-0.21 ± 0.02	2.343
VAAS	51.47 ± 0.20	9.46 ± 0.19	0.45 ± 0.02	2.342	51.31 ± 0.20	9.67 ± 0.20	0.50 ± 0.02	2.368
VIL0	48.15 ± 0.18	8.80 ± 0.18	0.24 ± 0.02	2.367	47.70 ± 0.19	9.17 ± 0.19	0.23 ± 0.02	2.249
VILL	28.89 ± 0.18	0.78 ± 0.18	-0.20 ± 0.02	2.249	29.25 ± 0.18	1.22 ± 0.18	-0.38 ± 0.02	2.256
VIS0	49.13 ± 0.19	8.56 ± 0.18	0.28 ± 0.02	2.255	48.68 ± 0.19	8.76 ± 0.19	0.26 ± 0.02	2.375
WARE	44.71 ± 0.19	8.00 ± 0.19	-0.16 ± 0.02	2.374	43.99 ± 0.20	8.33 ± 0.20	-0.21 ± 0.02	2.376
WROC	52.97 ± 0.19	9.75 ± 0.19	-0.12 ± 0.02	2.374	52.53 ± 0.19	9.92 ± 0.19	-0.23 ± 0.02	2.377
WSRT	45.96 ± 0.19	8.35 ± 0.19	-0.06 ± 0.02	2.375	44.75 ± 0.20	8.64 ± 0.20	-0.19 ± 0.02	2.400
WTZR	48.58 ± 0.17	8.95 ± 0.16	0.18 ± 0.02	2.399	48.45 ± 0.17	9.12 ± 0.17	-0.02 ± 0.02	2.238
ZECK	53.88 ± 0.14	6.75 ± 0.14	0.43 ± 0.02	2.237	54.42 ± 0.14	7.07 ± 0.14	0.38 ± 0.01	2.097
ZIMM	47.83 ± 0.15	6.74 ± 0.15	-0.03 ± 0.02	2.095	47.44 ± 0.16	7.24 ± 0.16	-0.14 ± 0.02	2.162

Atmos. Meas. Tech. Discuss., doi:10.5194/amt-2016-5, 2016
Manuscript under review for journal Atmos. Meas. Tech.
Published: 1 February 2016

Atmospheric Measurement Techniques Discussions

Table 3. Results of analysis of the 18 year ZTD time series from the first (Repro1) and the second (Repro2) EPN reprocessing campaigns

Station	Annual amplitude (mm)	Semiannual amplitude (mm)	Trend value (mm/decade)	ZTD Mean (m)	Annual amplitude (mm)	Semiannual amplitude (mm)	Trend value (mm/decade)	ZTD Mean (m)
	Repro1				**Repro2**			
BOR1	51.80 ± 0.17	9.62 ± 0.17	0.30 ± 0.0 2	2.385	51.29 ± 0.18	9.72 ± 0.17	0.27 ± 0.02	2.386
CAGL	37.88 ± 0.18	2.83 ± 0.17	0.16 ± 0.02	2.376	37.57 ± 0.17	2.53 ± 0.17	0.06 ± 0.02	2.376
DELF	43.76 ± 0.18	8.06 ± 0.18	0.01 ± 0.01	2.405	42.56 ± 0.19	8.52 ± 0.19	-0.14 ± 0.02	2.405
DENT	43.78 ± 0.19	7.89 ± 0.19	-0.05 ± 0.02	2.411	42.90 ± 0.19	8.26 ± 0.19	-0.12 ± 0.02	2.413
DOUR	43.50 ± 0.18	7.96 ± 0.18	-0.04 ± 0.02	2.346	42.83 ± 0.18	8.33 ± 0.18	-0.09 ± 0.02	2.347
EBRE	54.28 ± 0.20	9.13 ± 0.20	0.22 ± 0.02	2.424	53.74 ± 0.20	9.43 ± 0.20	0.13 ± 0.02	2.426
GOPE	48.45 ± 0.16	8.54 ± 0.16	-0.41 ± 0.02	2.255	48.47 ± 0.16	8.66 ± 0.16	-0.59 ± 0.02	2.256
GRAS	41.61 ± 0.16	3.13 ± 0.16	0.14 ± 0.02	2.054	41.45 ± 0.16	3.46 ± 0.16	0.00 ± 0.02	2.056
GRAZ	55.47 ± 0.15	8.39 ± 0.15	0.28 ± 0.01	2.281	55.35 ± 0.16	8.55 ± 0.15	0.19 ± 0.01	2.281
HERS	40.95 ± 0.20	8.28 ± 0.20	0.40 ± 0.02	2.405	39.98 ± 0.20	8.62 ± 0.20	0.31 ± 0.02	2.407
JOZE	52.77 ± 0.17	10.65 ± 0.17	0.36 ± 0.02	2.380	52.48 ± 0.18	10.38 ± 0.1	70.31 ± 0.02	2.379
KIRU	49.94 ± 0.17	11.14 ± 0.17	0.10 ± 0.02	2.253	49.68 ± 0.18	11.73 ± 0.1	70.10 ± 0.02	2.254
LAMA	51.76 ± 0.17	9.84 ± 0.17	0.42 ± 0.02	2.358	51.42 ± 0.18	9.89 ± 0.18	0.31 ± 0.02	2.359
MAS1	29.81 ± 0.17	7.47 ± 0.17	0.30 ± 0.02	2.392	29.63 ± 0.17	7.15 ± 0.17	0.09 ± 0.02	2.394
MATE	40.97 ± 0.16	0.62 ± 0.16	0.03 ± 0.01	2.283	40.91 ± 0.16	0.40 ± 0.16	0.01 ± 0.01	2.283
MEDI	54.09 ± 0.18	4.37 ± 0.18	0.15 ± 0.02	2.430	53.84 ± 0.18	4.60 ± 0.18	0.04 ± 0.02	2.432
METS	49.92 ± 0.18	9.76 ± 0.18	0.27 ± 0.02	2.360	49.55 ± 0.19	10.02 ± 0.1	90.29 ± 0.02	2.362
MOPI	49.14 ± 0.16	8.67 ± 0.16	-0.10 ± 0.02	2.257	49.68 ± 0.16	8.69 ± 0.16	-0.21 ± 0.02	2.262
ONSA	46.29 ± 0.18	8.91 ± 0.18	0.19 ± 0.02	2.390	45.66 ± 0.17	9.24 ± 0.19	0.19 ± 0.02	2.392
PENC	52.10 ± 0.16	8.74 ± 0.16	0.45 ± 0.02	2.350	52.04 ± 0.17	8.79 ± 0.16	0.28 ± 0.02	2.351
POTS	48.92 ± 0.17	8.77 ± 0.17	0.41 ± 0.02	2.377	48.21 ± 0.18	8.86 ± 0.18	0.32 ± 0.02	2.380
REYK	42.45 ± 0.21	6.59 ± 0.21	0.18 ± 0.02	2.352	41.38 ± 0.22	6.98 ± 0.21	0.10 ± 0.02	2.353
RIGA	52.72 ± 0.18	10.39 ± 0.18	0.50 ± 0.02	2.390	52.56 ± 0.19	10.51 ± 0.1	80.57 ± 0.02	2.392
SFER	24.21 ± 0.19	4.12 ± 0.19	0.18 ± 0.02	2.423	23.88 ± 0.19	3.89 ± 0.19	-0.01 ± 0.02	2.424
VILL	29.40 ± 0.17	1.08 ± 0.17	-0.16 ± 0.02	2.255	29.56 ± 0.17	1.52 ± 0.17	-0.30 ± 0.02	2.256
WARE	44.20 ± 0.18	8.20 ± 0.18	0.04 ± 0.02	2.374	43.48 ± 0.19	8.51 ± 0.18	0.03 ± 0.02	2.376
WTZR	48.17 ± 0.16	9.00 ± 0.15	0.34 ± 0.01	2.236	48.02 ± 0.16	9.13 ± 0.16	0.18 ± 0.02	2.238
ZIMM	47.37 ± 0.15	7.01 ± 0.14	0.12 ± 0.01	2.162	47.03 ± 0.15	7.49 ± 0.15	0.03 ± 0.01	2.162